Computational efficiencies and prediction accuracy of a physics-based building energy simulation tool for urban energy analysis

Richard C. Johnson[1], Mohammad Royapoor[2], Sara Walker[2]
[1]Dept. of Civil and Structural Engineering, University of Sheffield, Sheffield, UK
[2]Sir Joseph Swan Centre for Energy Research, Newcastle University, Newcastle, UK

Abstract

The decarbonisation of residential building stock in the UK requires accessible tools that can reliably and rapidly model residential building power demands as a function of multiple low carbon technologies and building control schemes. Whilst a variety of modelling tools exists, these platforms are either intended for expert analysts, are not suited to rapid simulation (and therefore cumbersome at stock modelling scale) or are not flexible enough to allow analysis of detailed active control schemes. This work builds on a previously developed dynamic domestic building modelling tool developed in MATLAB/Simulink environment and intended for rapid generation of electrified heat demand profiles in buildings. The number of parameter inputs and time-resource required to prepare EWASP tool is several order of magnitude smaller than an equivalent EnergyPlus model, computational efficiency of this tool as well as its prediction accuracy are benchmarked against an equivalent E+ model. The EWASP model required 13 times less parameter input, reducing analyst time requirement and human effort. Both models produced similar trends of loads against external climatic changes for a Passivhaus case-study fabric while overall EWASP generated smaller ASHP electrical loads (4.4 kWh·m^2·yr) than EnergyPlus model (5.8 kWh·m^2·yr) which will be examined in future works. EWASP tool can assist assessment of the impact of fabric or HVAC retrofit and design and control scenario in buildings on the local distribution network and wider power grid.

Introduction

The history of building energy modelling can be traced as far back as the dawn of personal computers in late 1960s, when a variety of response factor methods were used to perform transient heat flow calculations and automate building heating and cooling load calculations (Royapoor 2015). For most of the late 20th and early 21st century, the research work focused mostly on the improvement of energy models, visualisation of results, computational efficiencies and uncertainty treatment. A new paradigm however is emerging where the planning and operation of distributed multi-vector energy systems necessitates analysis of energy requirement of building clusters. This new trend is underwritten by the need to design and optimise operation of large scale storage, EV integration, renewable energy source (RES) shares to ultimately bring about low or zero carbon communities (De Jaeger 2020, Zhang 2018). This work aims firstly to presents a new first-principle based method for building energy simulation deployed in MATLAB/Simulink environment for rapid production of building stock demand profiles in order to assist assessment of the impact of fabric or HVAC retrofit and design and control scenario in buildings on the local distribution network and wider power grid. The main objective of this work is to provide a cross-validation of the simulation results of this first principle-based tool against an equivalent E+ model results. E+ is one of the most widely adapted tools for building energy simulation and extensively researched and assessed by the research community. This work outlines the comparative results of these two tools and discusses the computational efficiency and accuracy of the proposed new model, and the implications for rapid generation of thermal profiles, precision of results and their scalability.

Literature Review

Radical changes that are underway to decarbonise energy systems have made it necessary to understand energy systems at community level. While in most developed and developing countries energy systems are still planned and delivered in a centralised manner, regulatory forces such as he recast of the European Union Renewable Energy Directive (RED II) bring the focus increasingly onto a decentralised but integrated energy systems that can be optimised and managed at community level (Lowitzsch 2019). Stock modelling of the built environment have been undertaken from a top down or bottom up approach (De Jaeger 2020), and may or may not take heed of building characteristics (McCallum 2019). Bottom up approaches tend to use physics-based models (Royapoor 2019), metering data (Shahrokni 2014), an agent-based approaches (Nageli 2020) or indeed a hybrid approach that combines the certainty of field data and flexibility of physics-based models to derive new insights (Brøgger 2019). A degree of overlap exists between the bottom-up and top-down methods of stock modelling although the top down approach relies more on field data and empirical techniques whereas bottom-up solutions mostly rely on physics-based models (Johari 2020).

Conventionally building energy models were platforms to investigate multiple fabric and HVAC arrangements, building energy and environmental performance and

optimisation, occupant and daylight studies and decarbonisation efforts. Building models have also begun to be utilised in new areas, such as the assessment of integrating urban agriculture into buildings (Muñoz-Liesa 2020, Nadal 2017), assessment of buildings as a virtual power plant (Royapoor 2020), impact of pervasive sensor deployments (Clarke 2014)) and as mentioned previously city-scale energy modelling. A recent and widespread critic of these models is however lack of knowledge on inherent and systematic uncertainties of these models, as well as limited validation and calibration procedures (Johari 2020).

Water and air source heat pumps are mature technologies that have been in wide usage in both domestic and industrial applications due to their robust characteristics, efficiencies and wide availability. Heat pumps have gained considerable attentions as a decarbonisation tool (Royapoor 2019) and multiple theoretical or empirical models exists that describe their component-based mathematical representation either from a power flow or refrigerant cycle approach (Underwood, 2017). Theoretical models are mostly utilised for optimisation studies while empirical models are mostly suited to performance evaluation. As a function of being able to connect heating and power sectors while meeting thermal demand particularly when powered by renewables, heat pumps remain an instrumental part of future energy systems. The following section outlines the principles behind a high-fidelity model for the examination of heat pump characteristics at a single or a cluster of dwellings, as well as a description of E+ as benchmarking tool for the proposed model.

Methodology

EnergyPlus software descriptions

EnergyPlus (E+) is a heat balance-based building energy simulation programme capable of both heat and mass transfer calculations and is widely audited by the international research community (Royapoor 2015). The software can perform ventilation, lighting, heating and cooling and small power (and process) load computation in an integrated manner and generates results at a variety of user-specified intervals across the full annual cycle. Within this work E+ version 8.9 was used with DesignBuilder version 6.1 acting as E+ interface.

EWASP model and its configuration

An exemplar passive house building is modelled with a green roof, of the structure as defined in Feist (2019). Due to the large thermal mass of the roof structure, it is necessary to complete the modeling using a 3 node Beuken model (as opposed to a single U-value) as described by:

$$\begin{bmatrix} \frac{\partial T_{int}}{\partial t} \\ \frac{\partial T_{mid}}{\partial t} \\ \frac{\partial T_{ext}}{\partial t} \end{bmatrix} = \begin{bmatrix} -\frac{2U_{rf}}{{c_{rf}}^{1/3}m_{rf}} & \frac{2U_{rf}}{{c_{rf}}^{1/3}m_{rf}} & 0 \\ \frac{2U_{rf}}{{c_{rf}}^{1/3}m_{rf}} & \frac{-4U_{rf}}{{c_{rf}}^{1/3}m_{rf}} & \frac{2U_{rf}}{{c_{rf}}^{1/3}m_{rf}} \\ 0 & \frac{2U_{rf}}{{c_{rf}}^{1/3}m_{rf}} & -\frac{2U_{rf}}{{c_{rf}}^{1/3}m_{rf}} \end{bmatrix} \begin{bmatrix} T_{int} \\ T_{mid} \\ T_{ext} \end{bmatrix} + \begin{bmatrix} \frac{1}{c_{rf}m_{rf}} & 0 & 0 \\ 0 & \frac{1}{c_{rf}m_{rf}} & 0 \\ 0 & 0 & \frac{1}{c_{rf}m_{rf}} \end{bmatrix} \begin{bmatrix} \zeta_1 \\ \zeta_2 \\ \zeta_3 \end{bmatrix} \quad (1)$$

$$\begin{bmatrix} \zeta_1 \\ \zeta_2 \\ \zeta_3 \end{bmatrix} = \begin{bmatrix} [\alpha_{conv}(T_{zone} - T_{int}) + \alpha_{LW}(T_{zone} - T_{int})]A_{rf} \\ 0 \\ [(2.8 + 3v_{wind} + \alpha_{LW})(T_{out} - T_{ext}) + \dot{Q}_{SW}]A_{rf} \end{bmatrix} \quad (2)$$

The values U_{rf}, c_{rf} represent the roof total U value and specific heat capacity respectively, and take values of 0.1 W/m^{2}k with 1100 J/ kg K. being the total mass of roof material above the given building zone (m_{rf}). α_{conv} and α_{LW} are constants that represent heat transfer between the room and wall via convective and radiative heat transfer, $\dot{Q}_{SW}$ is solar irradiance on the roof external surface, which is modelled using global horizontal irradiance data for each timestep, and a surface albedo of 0.75. T_{zone}, T_{int}, T_{mid}, T_{ext}, are the zone, internal node, mid node, and external node temperatures respectively. v_{wind} is wind direction (in direction of travel), T_{out} is outdoor temperature, and A_{rf} is the area of the zone ceiling. Hence the left hand vector represents the change in temperature (per second) of each node.

The wall node is modelled using a Beuken model of the same type used to model the roof node, but with horizontal irradiance values replaced with 90° tilted values, and an individual profile assigned to each wall. North, east, west and south walls are modelled separately, even within the same zone. Walls are assigned a U value of 0.137 W/m^{2}k and a heat capacity (corrected for wall area) of 5.2x10^5 J/ m^{2}K, which represents the 2x150mm layers of EPS, 240mm lime sandstone, and 125mm of gypsum plasterboard, similar to the structure detailed in Feist (2019).

The floor node is modeled using a simple RC model; the floor slab is assigned a heat capacity, and heat can be gained from or lost to the ground, or the building interior. The U values for heat transfer are simply double the total U-value for heat transfer between the building interior and the ground, and takes a value of 0.113 W/m^{2}k, which represents a 100mm concrete slab atop 3 layers of EPS, as is typical in passive house design (Viking House 2020).

Roof U-value, U_{rf}	0.1 W/m^{2}k	**Floor U-value, U_{rf}**	0.113 W/m^{2}k
Roof heat capacity, c_{rf}	1100 J/ kg K	**Floor area corrected heat capacity, c_{rf}**	2.4x10^5 J/ m^{2}K
Wall U-value, U_{rf}	0.137 W/m^{2}k	**Infiltrative ACR @50Pa**	0.3/h (IPHA 2013)
Wall heat capacity, c_{rf}	5.2x10^5 J/ m^{2}K	**DHW tank Volume**	50 l/person
Thermostat setpoint	20^{o}C		

Table 1 – Thermo-physical parameter input for EWASP passivhaus model.

The heating system is assumed to consist of an air source heat pump serving radiators. Radiators are sized automatically using standard industry methods (CIBSE 2015), and heat pumps are sized to match the design heat output of the radiators. Mass flow rates are assigned to each radiator based on their volume and nominal output power capacity. Additionally, each radiator is assigned a thermostatic valve (TRV), that reduces, and eventually stops radiator flow across a range of user defined temperatures.

Heat loss/gain via infiltration and ventilation air flows between zones, and to the outside environment, is represented by pressure dependent terms for air flow through the building fabric ($\dot{m}_{n,out}$), flow between zones linked by open doors ($\dot{m}_{nm,op}$), zones linked by closed doors ($\dot{m}_{nm,cl}$), zones linked by a stairwell ($\dot{m}_{nm,str}$), and air flow extraction/addition via an MVHR system. Pressure dependent terms are modelled using airflow network method outlined in E+ Engineering Reference (EnergyPlus 2020) and the ASHRAE (2001) handbook, which are linearized if doing so results in insignificant changes in behavior from the original expression. The airflow problem is configured such that the net airflow into any given zone, n, must equal zero, in other words:

$$0 = \dot{m}_{n,out}(\Delta P_{n,out}, ELA) + \sum_{m=1}^{n_m} \dot{m}_{nm,op}(\Delta P_{nm}) + \sum_{m=1}^{n_m} \dot{m}_{nm,cl}(\Delta P_{nm}) + \dot{m}_{nm,str}(\Delta P_{nm}) + \dot{m}_{n,mech}(Occ, Vol) \quad (3)$$

$$\dot{m}_{n,mech} = \frac{0.3}{3600} vol_{tot} \frac{vol_n}{vol_{extract,tot}} X_{extract,n}\beta - \frac{0.3}{3600} vol_{tot} \frac{vol_n}{vol_{insert,tot}} X_{insert,n}\beta \quad (4)$$

$$\begin{cases} \beta = 0.7, if\ Occ = 0 \\ \beta = 1, if\ Occ \cdot 30 < 0.3 vol_{tot}, Occ \neq 0 \\ \beta = 1.3, if\ Occ \cdot 30 \geq 0.3 vol_{tot}, Occ \neq 0 \end{cases} \quad (5)$$

Where vol_{tot} is the total house volume, vol_n is the volume of zone 'n', $vol_{extract,tot}$ is the total volume of all zones from which air is extracted, and $vol_{insert,tot}$ is the same for all zones in which air enters. $X_{extract,n}$ and $X_{insert,n}$ are binary variables, and only one can take the value '1' at any given time (e.g. if the room is extracted from, then $X_{extract,n} = 1$ and $X_{insert,n} = 0$). Occ is the house occupancy number, and is equal to the current number of occupants.

The term $\frac{vol_n}{vol_{extract,tot}}$ calculates the fractional volume of each extraction zone relative to the total extraction zone volume, then $\frac{0.3}{3600} vol_{tot} X_{insert,n}\beta$ adjusts this fractional volume to give the amount of air that should be extracted in kg/s. The term β adjusts the extraction volume by ±30% based on house occupancy, and follows the logic outlined in Feist (2019), and IPHA (2013), which state that air changeover rate per hour should at least equal the minimum of 0.3 times the building volume, and $Occ \cdot 30$ when occupants are present, and continue at a 30% lower rate otherwise.

The temperature of air added to any zone can be calculated using,

$$T_{extract,n} = \sum_{n=1}^{n_{zones}} \frac{vol_n}{vol_{extract,tot}} X_{extract,n} T_{zone,n} \quad (6)$$

$$T_{insert,n} = (T_{extract,n} - T_{out})\eta_{MVHR} + T_{out} \quad (7)$$

Where η_{MVHR} represent the heat recovery efficiency of the MVHR system, and is set equal to 0.8. The equations effectively calculate the mass flow weighted average of the extraction room temperatures, then add a portion of the extracted heat to the inserted air (governed by η_{MVHR}). To prevent thermal discomfort in summer, the heat recovery system is disabled when outdoor temperature exceeds 18^{o}C.

Case-study platform and weather files

Due to the very tight thermal envelope, results are much more sensitive to internal gains than a typical UK residence, so care was taken to ensure these figures were sensible. Building occupancy is simulated using the CREST model (McKenna 2016), as are internal gains associated with occupants and appliances. However, the default active and inactive occupant gains are reduced slightly to 60 W/occupant (asleep) and 80 W/occupant (awake, mostly sitting and mild activity), which better represents human emissions when sedentary, and is better in line with PHPP9 (a validated industry standard package for passive house energy estimations). Furthermore, a constant heat loss of 25W/occupant is applied throughout the year to account for evaporative heat losses.

Latest CIBSE Test Reference Year (TRY) for Central Newcastle is utilised to input irradiance, wind speed, wind direction, outdoor air temperature, and ground temperature in both E+ and EWASP models.

Results and Discussion

EWASP results

Daily space heating demand peaks at 9 – 12 kWh on the coolest winter day and falls to zero between late April and the start of November.

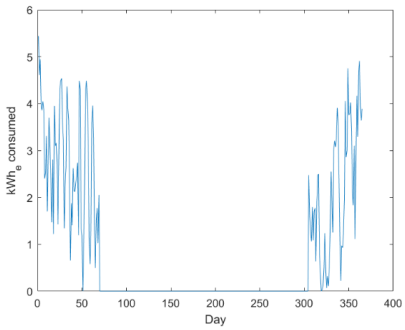

Fig 1 - total electricity consumed (for space heating only) by the heat pump on each day of the year.

Higher resolution results for a winter day (average temperature 4ºC) are shown in fig. 2. Whilst heat pump cycling behaviour is still visible, it is overshadowed by normal electrical demand (fig. 2, left). Heat pump cycles typically last 12 minutes, with a duty cycle of 50%, at times when space heating is required.

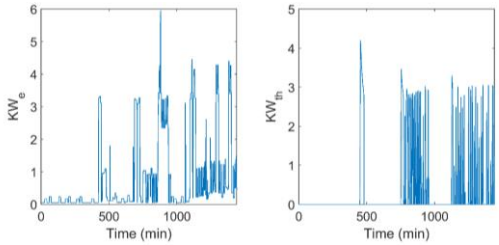

Fig 2 - (left) total electrical demand profile for one January day (right) heat delivered by the ASHP for space heating during the same day.

EWASP computational efficiency

The EWASP model runs at 5 second temporal resolution, and produces 1 day of output data in 18s. A 365-day time series of data can be generated in 5800s (this is lower per day than the 1-day case, as model does not have to be initialized at the beginning of each day). E+ on the other hand can perform simulations at designated timesteps of 1min to 1 hr. In order for E+ to perform a simulation at 1min intervals, weather files need to have a similar temporal resolution (as opposed to hourly weather files used in this study). This makes the comparison of simulation time for the geometry under assessment here incomparable because while 14 times quicker (see table 2), E+ was set up to perform an annual simulation at half hourly timesteps as opposed to 5 second that EWASP simulates at. However principally the advantage of EWASP is the ability of the analyst to set up a nominal model in a much shorter period than would be the case with E+. A fully characterised domestic building requires around 253 input parameters in E+, whereas EWASP can represents the same model with 20 input parameters. While the larger number of E+ parameter input space provides great flexibility for an advanced analyst, it also lent itself to errors, oversights, oversimplification or misrepresentation of the target building that in recent years has led to criticism of energy modellers (Imam 2017). The reduced parameter space of EWASP makes it more accessible to a wider community of modellers while minimising human error risks by offering a more compact set of input values. This also reduces the parameterisation time from several days to few minutes as E+ geometry creation and parameterisation for this case-study required 40 hours of an experienced analyst time, compared to 15 minutes for an EWASP model.

		EWASP	**EnergyPlus (E+)**
Parameterization	Weather Data	*CIBSE Current TRY (NWL)*	*Same*
	Building Fabric	*As outlined in Table 1*	*Same*
	Indoor conditions	*Time-dependent zone temp*	*Same*
	HVAC description	*Outlined in method*	*Outlined in EnergyPlus, 2020*
	Occupant behaviour	*Deterministic profiles*	*fractional schedules*
Computational	Engine	*Intel(R) Core ™ i5-8350U*	*Same*
	Operating system	*Windows 10*	*Same*
	Parameter inputs (no.)	*20*	*253*
	Parameterization time	*15 min*	*40 hours*
	Simulation time (Sec.)	5800	*405*
	Simulation output resolution	*5 seconds*	*30 mins*

Table 2 – Description of parameter input values and computational resources for EWASP and E+ models

ASHP results of EWASP benchmarked against E+

The EWASP model produces an air-source heat pump duty for annual space heating of 4.4 kWh/m^2/yr., while E+ model has a larger prediction of 5.8 kWh/m^2/yr (see table 3). In area weighted heating requirement (kWh/m^2/yr.) as well as total (kWh) and HH mean (W) over annual cycle the EWASP produces results that are 25% smaller. Interestingly, the instances when the Passivhaus remains in freefloat mode is also larger in EWASP model (89% in EWASP as oppose to 74% in E+). This indicates that the control schedule of E+ calls for ASHP action 15% more

frequently over half-hourly instances of annual cycle, and in doing so spreads the ASHP duty across a greater diurnal cycle. However, the greatest difference between the two models is the instances of maximum load which in the case of EWASP model is 998 W, while E+ produces a maximum load of only 337 W. These two maxima instances do not occur concurrently. These non-concurrent load profiles can arise from differences in zone temperature control schedules, occupant activity profiles, ASHP operational dynamics and fabric and infiltration loss calculations. Table 3 summarises the key comparative statistics of half-hourly instances of ASHP electrical duty from both models.

	EWASP	**E+**
Load instances (n)	17,520	17,520
Standardised heating demand (kWh.m^2.yr)	4.4	5.8
Sum (kWh)	317.89	419.37
% annual time of no duty	89%	74%
Maximum HH load (W)	998	337
Mean (W)	36.3	47.9
Std. Dev. (W)	116.6	55.4

Table 3 – Descriptive statistics of the ASHP electricity demand at half hourly intervals across the full annual cycle

In order to better illustrate the response of both models against the major determinant of the ASHP duty (which is the weather data), electrical AHSP duty of both models are plotted against weather data inputs to examine the sensitivity of models individually (Fig 3 - 5). Fig 3 demonstrated sum of all half hourly (HH) ASHP electrical duty for both models when plotted against advancing external air temperature at intervals of 1K. The correlation between sum of the loads predicted by both models is 96 %, quite understandably indicating a strong relationship between both model predictions. Interestingly while both models begin to generate results at -5°C, the Passivhaus model requires no heating at 13°C within E+ as opposed to 14°C within the EWASP model. The annual summation of all ASHP electrical loads (or the area underneath each line graph) is larger for EWASP model than E+ which is evident in Fig 4 as well.

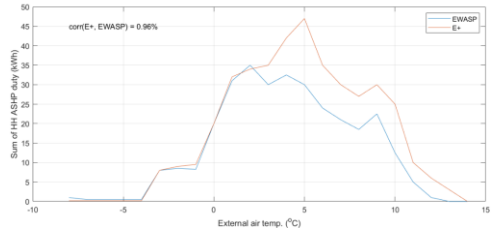

Fig 3 –Sum of all instances of half-hourly ASHP duties grouped against 1K-wide bands of external air temperature

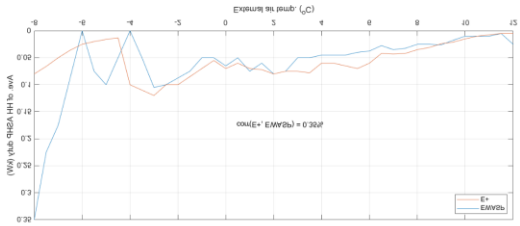

Fig 4 –Average of all instances of half-hourly ASHP duties grouped against 0.5K-wide bands of external air temperature

Fig 4 demonstrates that when examining the average of all HH loads against external air temperature, both models begin produce no load at external temperatures above 14°C. In other words, the Passivhaus dwelling enters a freefloat condition due to its highly insulated and air-tight fabric at and above external air temperatures of 14°C. While in magnitude the E+ model continues to produce higher loads on average, the average of trend of HH loads at temperatures above -4°C are similar, whereas at and below -5°C the prediction of models have a much more pronounced disagreement which leads to a weaker overall correlation value of 35% between EWASP and E+ predictions at average HH interval. A similar pattern can be observed when examining the average of all instances of half-hourly ASHP duties against diffused solar irradiance (Fig 5). At diffused solar irradiance values of less than 20 W/m^2, a greater disagreement of trends exists between average HH ASHP electrical loads across all annual instances. Both models interestingly however begin to predict a state of thermal neutrality (no requirement for ASHP heating duty) at diffused solar irradiance of above 190W/m^2.

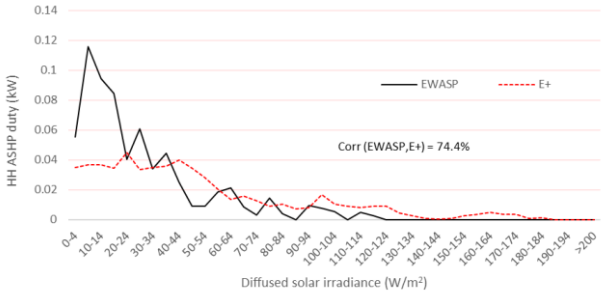

Fig 5 –Average of all instances of half-hourly ASHP duties grouped against intervals of diffused solar irradiance

As buildings are very complex thermo-physical entities with a wide number of interacting variables that interact in a complex yet fully intertwined manner to determine the heating load of the building at any given timestep . This chapter reported an initial set of comparative results which while showing a much simpler parameterisation of a building model using EWASP, yet at the same time larger perdition of ASHP duties for the target building. Further development of methodical comparative analysis is required to begin to quantify the impact of each category of parameter inputs, from occupancy schedules, ASHP characterisation and controls and ultimately the interpretation of building envelop and local climate within each model.

Limitations and future works

While the purpose of this study was not to achieve a perfect match between the predictions of the platforms examined, the disagreements in simulation results of the models leaves a wide scope of activities that can assist in quantifying the underlying differences of these simulation platforms. One approach is the investigation of the magnitude of change in the results of each model as a function of an input parameter adjustment, in other words a comparative sensitivity analysis to methodically examine if the models respond proportionally to changes in HVAC, fabric or occupant representations. In its fuller form - particularly where actual field data of a case-study building may be available - this comparative work can be undertaken via an uncertainty quantification with Bayesian statistics where a large number of simulations with changing input parameter (selected through hypercube sampling) can enable a sensitivity analysis and uncertainty treatment of both models.

Conclusion

Building energy simulation tools remain very effective platforms for decarbonisation of the built environment by enabling comparative appraisals of multiple technologies and design and topology configurations. While multiple platforms exist for building energy modelling analysis, some are models are only suitable for advance analysts and require considerable knowledge and expertise to fully parametrise, run and interpret the results. The work presented an early stage comparison between two tools, one developed for swift generation of first principle based ASHP duties (EWASP) and the other one of the most widely utilised and advanced building energy simulation platform (EnergyPlus). While EnergyPlus is heavily audited by the international research community and has been demonstrated to produce highly accurate results it required 253 different parameter inputs to complete a Passivhaus level case study building. This compared to 20 parameters within EWASP environment. This large reduction of the parameterisation space results in an analyst being able to produce ASHP results within a timespan that is several order of magnitude smaller than E+ and also subsequently less prone to human errors. This reduction of parameterisation space also allows faster representation of a cluster of buildings and hence much less cumbersome studies of urban scale energy impacts of a widescale adaption of ASHPs, retrofit measures, compliance and urban energy system planning. Across the full annual cycle and at half hourly intervals both models presented similar trends against the dynamics of external climate, however EWASP model produced generally smaller electrical loads that both against advancing intervals of external air temperature and external solar irradiance remained for most parts smaller than E+ predictions. These relate to fundamentally different modelling capabilities and modelling assumptions arising from very different component algorithms and parameter inputs. Future works can examine and characterise these underlying differences in a methodical manner using elements of Bayesian statistics and uncertainty treatment.

Acknowledgement

The authors wish to acknowledge funding from the Industrial Strategy Challenge Fund and Engineering and Physical Sciences Research Council, EP/S016627/1, for the Active Building Centre research project.

References

ASHRAE, *ASHRAE Handbook 2001 Fundamentals*. 2001: Atlanta, Ga.

Brøgger, M., P. Bacher, and K.B. Wittchen, *A hybrid modelling method for improving estimates of the average energy-saving potential of a building stock.* Energy and Buildings, 2019. **199**: p. 287-296.

CIBSE, *Guide A; Environmental Design*, in *1.4 Modelling thermal comfort*. 2015, The Chartered Institution of Building Services Engineers: London.

Clarke, J., et al., *Pervasive sensing as a mechanism for improving energy performance within commercial buildings.* Proc. Building Simulation and Optimization, 2014.

De Jaeger, I., et al., *A building clustering approach for urban energy simulations.* Energy and Buildings, 2020. **208**: p. 109671.

EnergyPlus Engineering Reference. *Airflow Network Model*. [cited 2020 24 Feb]; Available from: https://bigladdersoftware.com/epx/docs/8-3/engineering-reference/airflownetwork-model.html#airflownetwork-model.

EnergyPlus Engineering Reference, *The Reference to EnergyPlus calculations*. Version 8.9.0.

Feist, W., R. Pfluger, and W. Hasper, *Durability of building fabric components and ventilation systems in passive houses.* Energy Efficiency, 2019.

Imam, S., D.A. Coley, and I. Walker, *The building performance gap: Are modellers literate?* Building Services Engineering Research and Technology, 2017. **38**(3): p. 351-375.

IPHA. *Passive House Guidelines*. [cited 2013 8 July]; Available from: http://www.passivehouse-international.org/index.php?page_id=80.

Johari, F., et al., *Urban building energy modeling: State of the art and future prospects.* Renewable and Sustainable Energy Reviews, 2020. **128**: p. 109902.

Lowitzsch, J., C.E. Hoicka, and F.J. van Tulder, *Renewable energy communities under the 2019 European Clean Energy Package – Governance model for the energy clusters of the future?* Renewable and Sustainable Energy Reviews, 2020. **122**: p. 109489.

McCallum, P., et al., *A multi-sectoral approach to modelling community energy demand of the built environment.* Energy Policy, 2019. **132**: p. 865-875.

McKenna, E. and M. Thomson, *High-resolution stochastic integrated thermal–electrical domestic demand model.* Applied Energy, 2016. **165**: p. 445-461.

Muñoz-Liesa, J., et al., *Quantifying energy symbiosis of building-integrated agriculture in a mediterranean rooftop greenhouse.* Renewable Energy, 2020.

Nadal, A., et al., *Building-integrated rooftop greenhouses: An energy and environmental assessment in the mediterranean context.* Applied Energy, 2017. **187**: p. 338-351.

Nägeli, C., et al., *Towards agent-based building stock modeling: Bottom-up modeling of long-term stock dynamics affecting the energy and climate impact of building stocks.* Energy and Buildings, 2020. **211**: p. 109763.

Royapoor, M. and T. Roskilly, *Building model calibration using energy and environmental data.* Energy and Buildings, 2015. **94**(0): p. 109-120.

Royapoor, M et al., *Carbon mitigation unit costs of building retrofits and the scope for carbon tax, a case study.* Energy and Buildings, 2019. **203**: p. 109415.

Royapoor, M., et al., *Building as a virtual power plant, magnitude and persistence of deferrable loads and human comfort implications.* Energy and Buildings, 2020. **213**: p. 109794.

Shahrokni, H., F. Levihn, and N. Brandt, *Big meter data analysis of the energy efficiency potential in Stockholm's building stock.* Energy and Buildings, 2014. **78**: p. 153-164.

Underwood, C.P., M. Royapoor, and B. Sturm, *Parametric modelling of domestic air-source heat pumps.* Energy and Buildings, 2017. **139**: p. 578-589.

Viking House. *PASSIVE SLAB (INSULATED FOUNDATIONS)*. 2020 [cited 2020 24 Jun]; Available from: http://www.viking-house.ie/passive-house-foundations.html.

Zhang, X., et al., *A review of urban energy systems at building cluster level incorporating renewable-energy-source (RES) envelope solutions.* Applied Energy, 2018. **230**: p. 1034-1056.